

Smearing and its Effects on the Highest Optical Branch of Graphene

Onaiwu N. K.¹ and Idiodi J.O.A.²

¹Dept. Of Physics with Electronics, Crawford University, P.M.B. 2001, Faith-City, Igbesa, Nigeria

²Dept. Of Physics, Faculty of Physical Sciences, University of Benin, Benin City, Nigeria.

Abstract

The effects of smearing on the highest optical branch (HOB) in the phonon dispersion of graphene is looked at using the density functional theory (DFT) and the generalised gradient approximation (GGA) performed using the Quantum-ESPRESSO code. The calculated phonon dispersion is matched with some inelastic neutron scattering (INS) and inelastic X-ray scattering (IXS) experimental data. The crossing of the HOB at K is found to depend on the value of the Gaussian spreading used for the Brillouin-zone integration. While it is almost flat at for a large value, the situation is a little different for a very small value of the spreading.

1.0 Introduction

Graphene which is a single layer of graphite is at the verge of overtaking silicon in electronics applications. This is largely due to the ability to control the carrier density [1] an attribute which endows it with ballistic conduction at room temperature thereby making it a suitable material for both flexible transistors [2, 3, 4] and interconnects.

The dependence of the highest optical branch (HOB) on Kohn anomaly stems from the observation by Ref. [5] that electrons possess the ability to screen the ionic electric field due to the geometry of the Fermi surface. This screening, however, results in a change in the frequency of some phonon and consequently an increase in its dispersion.

The effects of smearing on the phonon dispersion of graphene will be examined using the exchange-correlation interaction. This will be treated with the generalised gradient approximation (GGA) which employs the Perdew and Zunger parameterization of the correlation energy[6]. The Calculations will be carried out within density functional theory (DFT) using the PWSCF code [7]. The interaction between electrons and ionic cores will be described by an ultra-soft pseudopotential of Ref. [8] and the wave function will be expanded using energy cut-off of 25 Ry. The smearing method described in Ref. [9] is used in the calculations with a degauss value (i.e. the value of the Gaussian spreading used for the Brillouin-zone integration) set to 0.007 Ry and $16 \times 16 \times 1$ Monkhorst-Pack grid used for the Brillouin zone sampling. In addition, an in-plane lattice constant a_0 of 2.461 Å and a large interlayer distance per lattice constant of 10 is used.

2.0 Method

The phonon frequencies $\omega(\mathbf{q})$ are determined by solving the secular equation:

$$\left| \frac{1}{\sqrt{M_s M_t}} C_{st}^{\alpha\beta}(\mathbf{q}) - \omega^2(\mathbf{q}) \right| = 0, \quad (1)$$

where the M_s and M_t are the atomic masses of atoms s and t respectively and the dynamical matrix is given as:

$$C_{st}^{\alpha\beta}(\mathbf{q}) = \frac{\partial^2 E}{\partial u_s^{\alpha}(\mathbf{q}) \partial u_t^{\beta}(\mathbf{q})}, \quad (2)$$

Corresponding author: Onaiwu N. K., E-mail: onaiwu.kingsley.nosa@gmail.com, Tel.: +2348062614040

u_s is the displacement of atom s in the direction α . The second derivative of the energy in (2) is the change in the force $F_t^\alpha(\mathbf{q})$ acting on atom t in the direction β due to a displacement of the atom s in the direction α :

$$C_{st}^{\alpha\beta}(\mathbf{q}) = \frac{\partial}{\partial u_s^{\alpha}} F_t^\beta(\mathbf{q}) \quad (3)$$

$$= {}^{el}C_{st}^{\alpha\beta}(\mathbf{q}) + {}^{ion}C_{st}^{\alpha\beta}(\mathbf{q}) \quad (4)$$

However it can be shown, see for example Ref. [10], that:

$${}^{el}C_{st}^{\alpha\beta}(\mathbf{q}) = \frac{1}{N_c} \left[\int \frac{\partial n(\mathbf{r})}{\partial u_s^{\alpha}(\mathbf{q})} \frac{\partial V_{ion}(\mathbf{r})}{\partial u_t^{\beta}(\mathbf{q})} d\mathbf{r} + \int n(\mathbf{r}) \frac{\partial^2 V_{ion}(\mathbf{r})}{\partial u_s^{\alpha}(\mathbf{q}) \partial u_t^{\beta}(\mathbf{q})} d\mathbf{r} \right], \quad (5)$$

Where $V_{ion}(\mathbf{r})$ is the bare ionic (pseudo) potential acting on the electrons. The quantities $n(\mathbf{r})$ and E require a sum over an infinite number of \mathbf{k} . For metals, at $T = 0$, this corresponds to an integral over all wave-vectors contained within the Fermi surface which can lead to self-consistency field (scf) convergence problem. However, this can be resolved through "smearing".

Using the GGA pseudopotential C.pbe-rrkjus.UPF with the other parameters as specified in the introduction, the equilibrium lattice constant of 2.461 Å was obtained as shown in Fig. 1. This pseudopotential is our preferred choice since it reproduces the experimental data more closely [11]. As graphene is neither an insulator nor a metal, Methfessel and Paxton smearing [9] was used with a very small (0.007 Ry) degauss value. The result of the calculation is shown in Fig. 2. Obviously the HOB has been exaggerated at its crossing at K. If we follow the trend of the curve (the broken line), it is obvious that the branch is most likely to cross K at a much lower frequency.

Consequently, we increase the degauss value to 0.2 Ry and retain all the other parameters as in the previous calculation to see whether it can have any effect on the HOB and its crossing at K. The result of the calculation is shown in Fig. 3. The branch is almost at K and the crossing (phonon frequency) of this branch at Γ is also affected.

3.0 Results and Discussion

Fig. 1 shows the result of the optimisation of the energy with respect to a_0 . The optimised lattice constant $a_0 \approx a_{th}$, the theoretical value. The solid line is the calculated values while the dashed-line is the smoothed data. The minimum of the energy obviously is 2.461 Å or 4.6525 Bohr.

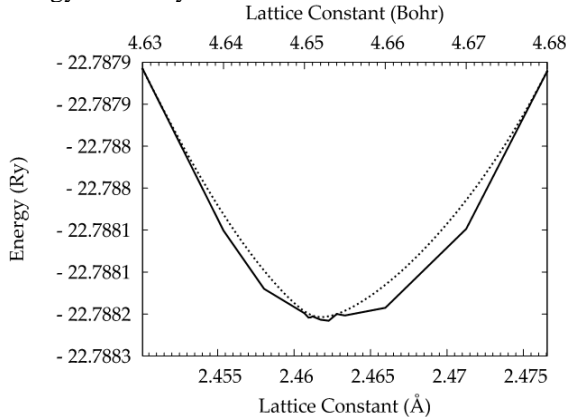


Figure 1: Minimization of the energy with respect to the equilibrium lattice constant a_0 . The solid line is the calculated values while the dotted-line is the smoothed data. The minimum of the energy obviously is 2.461 Å.

The phonon dispersion of graphene is shown in Fig. 2. The open circles and the triangles are the INS and IXS data of references [12, 13] respectively while the solid lines are current work. The inset shows the crossing of the HOB at K and the trend line that had been included to show the amount by which the branch has been affected by Kohn anomaly. The crossing of the HOB at K is $\approx 1315 \text{ cm}^{-1}$. However, the trend line shows that this branch is likely to cross at $\approx 1215 \text{ cm}^{-1}$. Since the calculation result is not in any way near this value, suggests that DFT is inadequate for predicting the crossing of the HOB at K.

The result of the calculation done with a degauss value of 0.2 Ry is shown in Fig 3. Obviously, the HOB is almost at and crosses K at $\approx 1362 \text{ cm}^{-1}$. This is not surprising as a high value of degauss is usually employed for metallic materials.

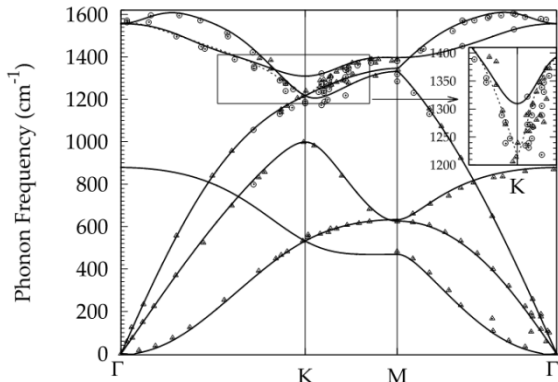


Figure 2: Phonon dispersion of graphene. The open circles and the triangles are the INS and IXS data of Refs. [12, 13] respectively while the solid lines are current work. The inset shows the crossing of the HOB at K and the trend line, shown here as dotted, that had been included to show the amount which the branch has been affected by Kohn anomaly.

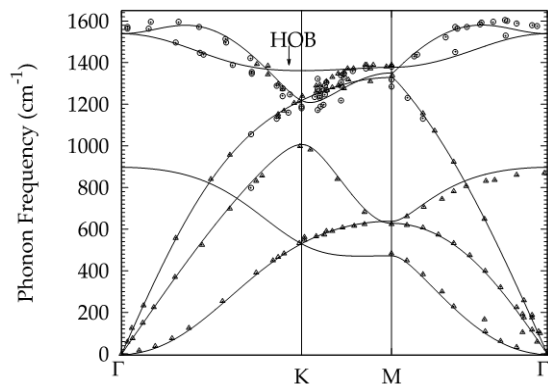


Figure 3: Phonon dispersion of graphene obtained following an increase in the value of the degauss to 0.2 Ry. The HOB is almost flat this time. The open circles and the triangles retain their definitions as in Fig. 2.

4.0 Conclusion

We have looked at the effects the value of the Gaussian spreading used for the Brillouin-zone integration have on the phonon dispersion of graphene using the exchange-correlation interaction and the way that this value affects the crossing of the HOB at the high-symmetry point K. Methfessel-Paxton smearing was employed and various values of degauss was applied. It is found that if a high

value of degauss is applied, the crossing of the HOB at K is higher than that observed for a much lower value.

In addition, the HOB is completely at in the neighbourhood of K contrary to the observation for very small values of the smearing parameter. This is however due to the fact that graphene is a semi-metal. So that a very high value of degauss is tantamount to treating graphene as a metal and a non-finite value is taking it to be a non-metal. Having said that, our result did not give the correct crossing of the HOB at K (see for example reference [14]) as our calculation did not take into cognizance the long range electron-electron correlation effects.

5.0 References

- [1]. K. S. Novoselov, A. K. Geim, S. V. Morozov, D. Jiang, M. I. Katsnelson, I. V. Grigorieva, S. V. Dubonos, and A. A. Firsov. Electric Field Effect in Atomically Thin Carbon Films. *Science*, 306:666{669, 2004.
- [2]. S. Cedric, A. Florence, L. Sylvie, T. S. Jung-Woo, C. H. Mark, D. Gilles, H. Henri, and D. Vincent. Flexible Gigahertz Transistors Derived from Solution-Based Single-Layer Graphene. *NanoLett.*, 12:1184, 2012.
- [3]. F. Schwierz. Graphene transistors. *Nature Nanotechnology*, 5:487, 2010.
- [4]. F. Xia, D. B. Farmer, Y-M. Lin, and Ph. Avouris. Graphene field-effect transistors with high on/off current ratio and large transport band gap at room temperature. *Nano Lett.*, 10:715, 2010.
- [5]. W. Kohn. *Phys. Rev. Lett.*, 2:393, 1959.
- [6]. J. P. Perdew, K. Burke, and M. Ernzerhof. Generalized Gradient Approximation Made Simple. *Phys. Rev. Lett.*, 77:3865, 1996.

- [7]. P. Giannozzi, S. Baroni, N. Bonini, M. Calandra, R. Car, C. Cavazzoni, D. Ceresoli, G. L. Chiarotti, M. Cococcioni, I. Dabo, A. Dal Corso, S. Fabris, G. Fratesi, S. de Gironcoli, R. Gebauer, U. Gerstmann, C. Gougoussis, A. Kokalj, M. Lazzeri, L. Martin-Samos, N. Marzari, F. Mauri, R. Mazzarello, S. Paolini, A. Pasquarello, L. Paulatto, C. Sbraccia, S. Scandolo, G. Sclauzero, A. P. Seitsonen, A. Smogunov, P. Umari, and R. M. Wentzcovitch. The quantum-espresso code. World Wide Web, <http://dx.doi.org/10.1088/0953-8984/21/39/395502>, 2009.
- [8]. M. Rappe, K. M. Rabe, E. Kaxiras, and J. D. Joannopoulos. Optimized Pseudopotentials. *Phys. Rev. B*, 41:1227, 1990.
- [9]. M. Methfessel and A. T. Paxton. High-Precision Sampling for Brillouin-Zone Integration in Metals. *Phys. Rev. B*, 40:3616, 1989.
- [10]. P. Giannozzi, S. de Gironcoli, P. Pavonne, and S. Baroni. Ab initio calculation of phonon dispersion in semiconductors. *Phys. Rev. B*, 43(9):7231, 1991.
- [11]. K. N. Onaiwu and J. O. A. Idioidi. Phonon Dispersion of Graphene-Effects of Pseudopotential. *IOSR-JAP*, 6:27{33, 2014.
- [12]. J. Maultzsch, S. Reich, C. Thomsen, H. Requardt, and P. Ordejón. Phonon Dispersion in Graphite. *Phys. Rev. Lett.*, 92:075501(4), 2004.
- [13]. M. Mohr, J. Maultzsch, E. Dobardžić, S. Reich, I. Milošević, M. Damnjanović, A. Bosak, M. Krisch, and C. Thomsen. The phonon dispersion of graphite by inelastic x-ray scattering. *Phys. Rev. B*, 76:035439, 2007.
- [14]. M. Lazzeri, C. Attacalite, L. Wirtz, and F. Mauri. Impact of the electron-electron correlation on phonon dispersion: Failure of LDA and GGA DFT functionals in graphene and graphite. *Phys. Rev. B*, 78:081406(R), 2008